Hindawi
Applied Computational Intelligence and Soft Computing
Volume 2022, Article ID 1996410, 13 pages
https://doi.org/10.1155/2022/1996410

Research Article

The Performance of a New Heuristic Approach for Tracking Maximum Power of PV Systems

Apripriharta Apripriharta,[1,2] Kusmayanto Hadi Wibowo,[1] Irham Fadlika,[1,2] Muladi Muladi,[1,2] Nandang Mufti,[2,3] Markus Diantoro,[2,3] and Gwo-Jiun Horng[4]

[1]*Department of Electrical Engineering, State University of Malang, Malang, Indonesia*
[2]*Center of Advanced Materials for Renewable Energy, Malang, Indonesia*
[3]*Department of Physics, State University of Malang, Malang, Indonesia*
[4]*Department of Computer Science and Information Engineering, Southern Taiwan University of Science and Technology, Tainan, Taiwan*

Correspondence should be addressed to Apripriharta Apripriharta; apripriharta.ft@um.ac.id

Received 19 May 2022; Revised 27 October 2022; Accepted 10 November 2022; Published 26 November 2022

Academic Editor: Bhargav Appasani

This paper presents a new heuristic method for maximum power point tracking (MPPT) in PV systems under normal and shadowing situations. The proposed method is a modification of the original queen honey bee migration (QHBM) to shorten the computation time for the maximum power point (MPP) in PV systems. QHBM initially uses random target locations to search for targets, in this case, MPP. So, we adjusted it to be able to do MPP point quests quickly. We accelerated the mQHBM learning process from the original randomly. We had fairly compared the mQHBM with several heuristics. Simulations were carried out with 2 scenarios to test the mQHBM. Based on the simulation results, it was found that mQHBM was able to exceed the capabilities of other methods such as original QHBM, particle swarm optimization (PSO) and perturb and observe (P&O), ANN, gray wolf (GWO), and cuckoo search (CS) in terms of MPPT speed and overshoot. However, the accuracy of mQHBM cannot exceed QHBM, ANN, and GWO. But still, mQHBM is better than PSO and P&O by about 15% and 18%, respectively. This experiment resulted in a gap of about 2% faster in speed, 0.34 seconds better in convergence time, and 0.2 fewer accuracies.

1. Introduction

Solar power systems offer environmentally friendly solutions, free and abundant resources, and economical and efficient PV panel technology [1]. The power generated by the solar panel is not flat but depends on the solar irradiation and the temperature on the surface of the panel. The output characteristic curve of the solar panel shows the maximum power at a certain point called the maximum power point P_{MPP} as shown in Figure 1. Electrical energy can be extracted optimally if the PV operates at the MPP point.

The maximum power point tracking (MPPT) method has developed rapidly to date [1–3]. The earliest ones, classical MPPT, such as FOC and FSC tracks V_{MPP} using $K_V V_{OC}$ and I_{MPP} with $K_I I_{MPP}$, respectively. They are the simplest MPPTs ever. If we look at the curves in Figures 1(a) and 1(b), the P_{MPP} location is reached when the PV terminal voltage V_{MPP} is less than the open circuit voltage V_{OC}, and the electric current coming out of the PV, I_{MPP} is smaller than the short circuit current (I_{SC}). Thus, they are easy to implement, cost-effective in computation, and suit the minimum systems. However, these methods are less accurate and inefficient for both normal and shaded conditions [3].

Changes in the external environment due to weather can cause an increase in temperature so that there can be hotspots on the PV, shadows that cover part or all of the PV surface, or dust on the PV surface, all of which can change the characteristics of the installed PV module. In specific, a more complex problem occurs when the irradiation is not

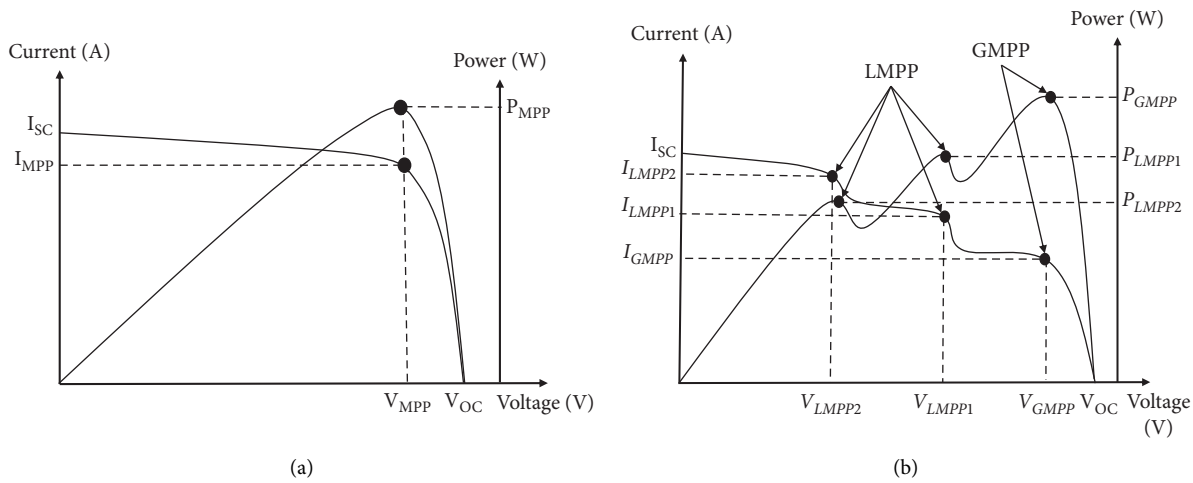

Figure 1: PV characteristics. (a) Normal condition, (b) shading condition.

linear due to the influence of the shadow on the PV surface, which results in several peaks, i.e., a local maximum (LMPP) and a global maximum (GMPP) on curvature, see Figure 1(b). MPPT must be able to find and track GMPP in various conditions to increase efficiency. Traditional heuristic methods with hill climbing (HC), such as perturb and observed (P&O) and incremental conductance (INC), are not reliable enough, often oscillate when there is a sudden change in irradiation, and are easily trapped in the LMPP [1, 2].

Heuristic or metaheuristic, which is sometimes called soft computing or artificial intelligence techniques for MPPT [1], consists of, i.e., artificial neural network (ANN) [4–6], fuzzy [7–10], particle swarm optimization (PSO) [7, 11–19], gray wolf optimization (GWO) [20–23], cuckoo search (CS) [23, 24], and queen honey bee migration (QHBM) [25, 26]. Moreover, MPPT with the original QHBM has only been tested on a normal system [26]. Heuristic MPPTs have fast convergence speeds, small oscillations, and good tracking rates in both normal and shaded conditions. The main drawback is that computation is expensive and complicated, so it requires higher costs than the classic MPPT. Various arguments and open debates about the performance of the MPPT method are discussed in a simulation framework.

Hybrid MPPT has been introduced in the literature, namely hybrid PSO and differential evolution (DE) [11], hybrid P&O and PSO [7, 16–18], and hybrid PSO with MVP [19]. Fuzzy [7–10] is mostly used in hybrid mode with other algorithms, both classic MPPTs [7] and more modern ones such as PSO [8] and cuckoo search (CS) [9]. CS used a special feature called "long jump" to avoid LMPP while at the same time shortening the tracking time required to reach GMPP in many cases [24]. In [23], the authors combined bat algorithm (BA) with CS to improve MPPT performances where several LMPP shorted to GMPP. In addition, ant colony [27], artificial bee colony [28], flying squirrel search optimization [29], and simulated annealing [30] demonstrated MPPT on PV systems.

We demonstrated QHBM with simulation and implementation on hardware, which is quite successful under normal conditions [26]. However, QHBM also encountered practical problems when implemented to deal with shadow problems or sudden changes in irradiation. Instead of running the MPPT heuristics alone, some researchers choose to combine them with the classic method. Generally, in this hybrid technique, the heuristic method will only be activated under certain conditions, including shaded states. Another mechanism is to optimize the classic MPPT parameters with the heuristic techniques mentioned earlier to increase MPP search performance [5].

In this paper, we demonstrate a modification of the QHBM, known as mQHBM, to search for MPP under normal and shaded conditions. The costly computation could be reduced by simplification, such that the boundary condition limits parameters, simplifies optimization functions, or changes decision-making; thus, we can apply heuristics to MPPT in low-cost devices. This paper focuses on addressing the MPP search problem under shadowing conditions in the PV system. We highlight our work in this paper as follows:

(i) In short, we modified the original QHBM to aim to speed up the computation and save memory by determining the decision criteria for searching MPPT under both normal and shadowing cases.

(ii) We conducted demonstrations through simulations on several scenarios to compare mQHBM performance with the original QHBM [25], ANN, PSO, GWO, CS, and traditional heuristic P&O in terms of tracking speed and accuracy of MPPT.

(iii) We implemented the mQHBM-MPPT to control a cûk converter for harvesting the maximum power from solar panels loaded with resistive loads. Then observe the results of performance tests in several scenarios.

The main difference between the mQHBM and the original QHBM [25, 26] is introduced twofold. First, there is the purpose of migrating the queen bee, and second, its nest coordinates were determined at the beginning. The MPP

value from the datasheet is used for the initial conditions of the iteration, and then the sensor system will read the position of the MPP change. The goal is to speed up iterations by minimizing agents or scouts so that the computing process can be faster and save memory. The MPP search process on mQHBM is still the same as the original QHBM [25], where the queen bee will be assisted by a scout in 8 cardinal sectors. This condition is repeated until the MPP value is obtained.

The rest of the paper is organized into five sections as follows: Section 2 details the PV model, the MPP concept, and the methods. Section 3 details the proposed mQHBM for MPP and the system under study. Section 4 is the result and analysis. At last, the paper concludes in Section 5.

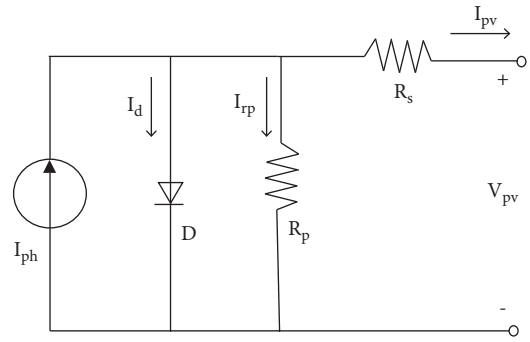

Figure 2: PV equivalent circuit.

2. Related Works

2.1. PV Model. PV panel consists of n solar cells. The circuit model for the PV panel is shown in Figure 2.

The diode current is obtained from the Shockley equation, namely.

$$I_{pv} = I_{ph} - I_D\left(e^{\left(V_{pv}+I_{pv}\cdot R_s/\eta\cdot V_t\right)}\right) - \frac{V_{pv} + I_{pv}\cdot R_s}{R_p}, \quad (1)$$

where I_o is the reverse saturation current, T is the cell temperature, q is the charge carrier, k is the Boltzman constant, and n is the ideality factor. The PV module has two limiting parameters (Figure 2), there are open circuit voltage (V_{oc}) and short-circuit current (I_{sc}). I_{sc} is obtained by setting $V = 0$ and $I_{sc} = I_{ph}$, where this value changes in proportion to the radiation of the cell. Besides, V_{oc} is the voltage on the PV terminal while the current IL = 0, then (1) leads to

$$V_{oc} = \frac{nkT}{q}\ln\left(\frac{I_D}{I_0}\right). \quad (2)$$

2.2. MPPT Methods

2.2.1. Concept of MPP Search. The main parameters of PV panels are open voltage, short circuit current, and peak power. The maximum power point (MPP), P_{mpp} is the point where the voltage (V_{mpp}) and current (I_{mpp}) on the PV terminal produce the maximum power. This condition is met by the maximum power theorem, so that the input resistance, $R_{in} = (V_{MPP}/I_{MPP})$ is equal to the load resistance R_L.

$$\frac{d(VxI)}{dt} = 0,$$
$$V_{mpp} = V_{OC} - \frac{kT}{q}\ln\left[\frac{V_{mpp}}{(nKT/q)} + 1\right]. \quad (3)$$

The product of V_{mpp} and I_{mpp} is related to the fill factor of PV systems.

A PV panel or module has characteristics defined by I–V and P–V curves, which are drawn at a specific value according to its parameters. Figure 1(a) shows the characteristics of a PV panel under normal conditions (STC), where the incident light is 1000 W/m^2, the temperature is 25°C, and the air mass is 1.5. In STC, the maximum power P_{mpp} is pointed out by single V_{mpp} and I_{mpp} points. To increase the current capability, the PV panel must be installed in parallel. On the other hand, series connections could increase the voltage capability of a PV system. In practice, the series-parallel connection is widely used for many applications.

Due to environmental changes, such as shadows on the PV surface and dust, the characteristics of the PV system also change, as depicted in Figure 1(b). Several P_{mpp} points may exist that consist of a global peak and a local peak. The problem with MPPT is that the load requires a constant voltage or current, so it is quite difficult to adjust the load impedance with MPPT. The dc-to-dc converter can be used to execute the MPPT task of matching the PV resistance to resistance [31–34].

2.2.2. Simple or Classic MPPT. The simple method for approaching the MPP is by using fractional open voltage (FOV), fractional short circuit (FSC), and hill climbing (HC). They defined the constant for voltage or current, respectively, which may reach the MPP point. This method is simple and requires the very least computation. Figure 3 displays the simple FOV, FSC, and HC MPPTs tried to reach MPP using constant k, which commonly ranges from 0.65 to 0.75. The FOV MPPT reaches the MPP through open panel voltage, which is practically used to switch the open and closed connection between the panel and load. Besides, the FSC-MPPT has to get the I_{SC} value by shorting the terminal. These methods are effective for low- to medium-power applications but not for large systems.

A systematic review of HC was presented in [1, 3]. P&O and IC are the mostly known HC- MPPT. At the peak of PV curve (Figure 3), dP/dV is equal to 0, before V_{mpp} is $dP/dV > 0$, after V_{mpp} is dP/dV. P&O approaching the peak by comparing the updated dP/dV until 0 or close to 0. I&C approached MPP using dI/dV and compared the updated value with $-I/V$. For the shadowing cases or sudden changes in irradiation, hill climbing methods tend to oscillate around the peak or even to a false peak.

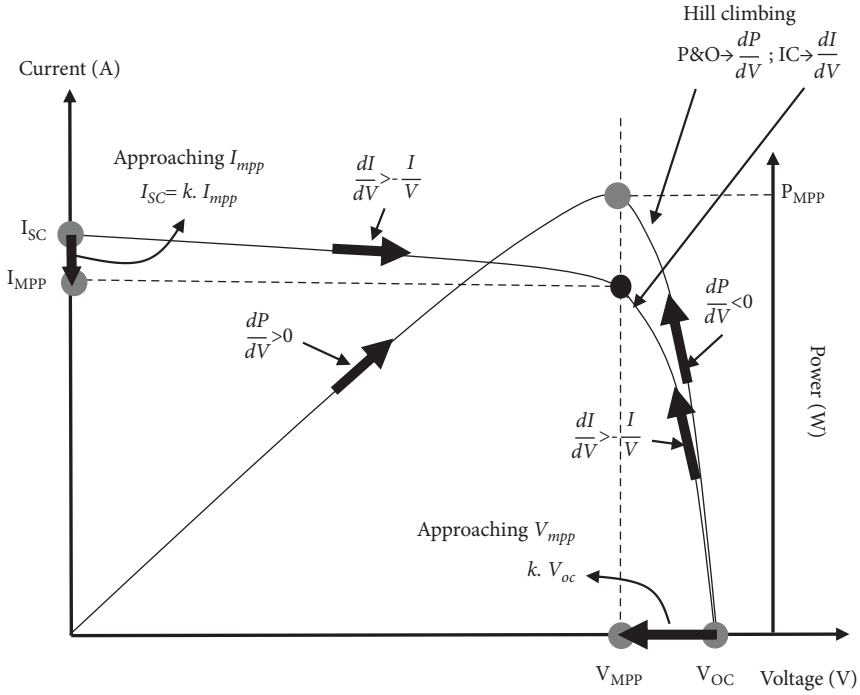

Figure 3: MPPT under normal conditions.

2.2.3. Heuristic Search. Various heuristic MPPT methods have been established in the literature [1–30]. Commonly, they are combined with the classic algorithm to enhance the performances of MPPT under shading conditions, see Figure 4. Each technique has its advantages and disadvantages, but based on general heuristics, MPPT can converge quickly and has high efficiency compared to conventional MPPT. However, heuristic MPPT is computationally intensive and expensive to implement. The hybrid method with conventional MPPT is more advantageous in terms of the balance between performance and complexity and combines the advantages of each. Some of the AI techniques used as MPPT include FLC [8], GA [1], and ANN [1, 4–6]. ANN is used to train and test the non-linear relationship between I–V and P–V. ANN takes input in the form of input current, input voltage, radiation, and temperature and then actually learns to adjust the behaviour of the solar system to achieve MPP [1]. FLC can be modified using ANN, with higher accuracy and simpler implementation [9].

GA [1] is widely used in MPPT to calculate the reference voltage of PV panels by modifying the population of individual solutions. GA produces relatively small oscillations, fast convergence, and dynamic speed. However, GA is not recommended for optimizing very large-scale, very complex, and big problems because of its simplified algorithm. In MPPT, GA is initialized by starting this trial parent population as an array.

Cuckoo search bee colony and ant colony which are well established and applied to various applications. PSO, GWO, and cuckoo search are most commonly used for MPPT, along with other methods such as FOV, FSC, IC, and P&O. Under normal conditions, this hybrid technique uses conventional methods to track MPP. In shaded conditions or

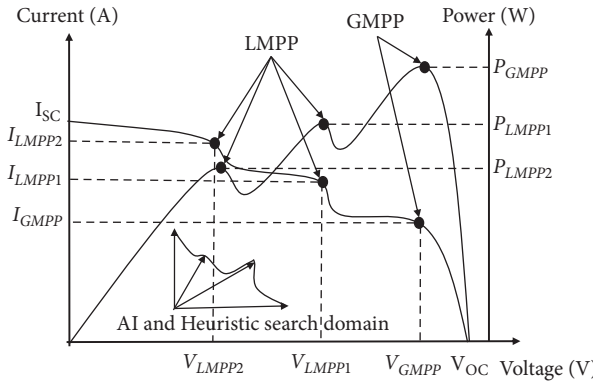

Figure 4: MPPT under shading conditions.

extreme weather, hybrid techniques will activate PSO, GWO, or others as MPPT. This combination can speed up the hybrid method for tracking GMPP in extreme weather conditions [1].

GWO [20–23] is a modern heuristic technique that imitates the natural behaviour of a herd of grey wolves. In the herd, there is a hierarchy of leaders, from highest to lowest, each defined by a different variable. GWO-MPPT works by obeying orders and viewing priority orders. The agents in the form of wolves are not very numerous, and they can search for prey in large areas. In MPP search, the hunting area is restricted, and LMPP and GMPP can be assessed as a priority, so GWO-MPPT works both in normal and shaded conditions. However, both the GWO and in cuckoo search each imitate the behaviour of the grey wolf and the cuckoo hunt, respectively. In both of these methods, the number of particles (agents) is less than in PSO, so the computation is faster.

2.2.4. QHBM. QHBM is one of the heuristic techniques published in 2017 to handle hotspots on WSN [25]. QHBM imitates the behaviour of a honey bee queen, who will naturally migrate in dangerous conditions as depicted in Figure 5. This behaviour also appears in the bee' princess (to simplify the story we called it queen). The queen will leave the nest and move from one place to another until the scouts find the right food location and she feels comfortable where she last visited to make a new nest [25].

The migration of the queen is random but deliberately limited to 8 cardinal sectors. The queen will make her decision by studying the code of the scouts within her sight. The queen uses the information from the scout to choose the direction to take next. And so on until the queen finds a place that is considered suitable for building a nest [25].

Step 1. Initialization. Figure 6 shows the logical view of the QHBM initialization process. The queen is in the center, and the scouts are spread randomly inside or outside sectors. The cardinal direction is pointed toward the destination pole. In the case of MPPT, these 8 possible poles are assigned as the $P_{Q(k+1)}$ and the queen is initially located at $P_{Q(k)}$. P_Q is the current value of PV system wattage obtained from sensors, k is the current iteration, and $k+1$ is the next iteration [25].

Step 2. Iteration. The iteration process of QHBM consists of several tasks, namely: deciding the moving direction, sector selection, choosing the pole (destination), calculating the distance travelled by Queen, and updating the queen position. There are several parameters used when applying this natural behaviour mathematically, namely destination, initial position, which could be 1D, 2D, or 3D, or more, and the weight of the information from the scouts. The decision is taken by using the probability, or percentage, of scouts in each sector, C_j. Each migration is determined by the radius of the journey, r. Naturally, the queen bee does not move as far as r but will stop at a certain point according to the size of the disturbance that may exist. This condition is repeated until the queen found places for a new hive [25].

$$C_k = \frac{1}{n}\sum_{k=1}^{n} e_{r(k)}, \tag{4}$$

$$p_k = \frac{C_k}{\sum_{k}^{8} = 1C_k}, \tag{5}$$

$$r_{k+1} = r_k(1-\alpha), \tag{6}$$

$$\begin{aligned} V_{Q(k+1)} &= V_{Q(k)} + r_{k+1}.\cos\theta_{k+1}, \\ P_{Q(k+1)} &= P_{Q(k)} + r_{k+1}.\sin\theta_{k+1}, \end{aligned} \tag{7}$$

$$g_m^{(k+1)} = g_m^{(k)}.\mathrm{rand}(\alpha), \tag{8}$$

where C_j, p_k, n, k, g_m, α, $e_{r(j)}$, are scout excitement value, sector probability, number of scouts, iteration, natural factors for learning, and residual energy, respectively. $P_{Q(k)}, P_{Q(k+1)}, V_{Q(k)}, V_{Q(k+1)}$ are the current and future values of the queen as they coordinate on the PV curve [25].

Stopping Criterion. For MPPT, we used epsilon $\varepsilon = 0\,001$. In the case of non-linear or shaded conditions, QHBM is also able to search quickly, even though it requires a large processor and memory like other heuristics. To save computations so that they can be applied to minimum processor devices, we made some modifications to the original QHBM [25]. The modified QHBM, or mQHBM, will be discussed in Section 3.3.

2.3. Cûk Converter. The loads applied to the PV require a constant current or voltage, so to adjust the resistance to the PV resistance, an interface in the form of a dc-dc converter is required. In this way, the impedance matching between PV and load can be obtained as a function of the duty cycle [1]. To keep the load feeling the maximum power, the dc-dc converter will adjust the duty cycle so that the PV input resistance is equal to the load resistance.

The output voltage of cûk converter in Figure 7 is given by

$$V_0 = \frac{d}{1-d}V_i, \tag{9}$$

and the PV resistance at MPP given by

$$R_{mpp} = \frac{(1-d)^1}{d^2}R_L. \tag{10}$$

3. Method

3.1. System Modelling. Simulations were carried out using the circuit in Figure 8 to study the performance of the mQHBM heuristic approach in finding MPP. This circuit uses a SRM50D 50Wp PV with specifications as shown in Table 1. The Cûk converter is used as a power interface for mQHBM-MPPT. The parameter specifications of the converter used in the test circuit are shown in Table 2. A bulk resistor is used as a dc load. Table 3 is a general table of parameters for control and epsilon.

3.2. The Proposed mQHBM. The proposed mQHBM block is equipped with voltage and current sensors. The voltage sensors are used to read the solar panel output voltage and load voltage in real time. The solar panel output current and load current are monitored in real time by the current sensors. The values of the voltage and current are then used as input for the computation of the MPP search process by mQHBM. Figure 8 shows that the mQHBM output is connected to the PWM block to produce an appropriate duty cycle to extract maximum power from the solar panel. To reduce the computation, we modified QHBM to mQHBm as follows:

(i) We consider the α as a random value (0 to 1) directly without updating the natural factor g_m.

(ii) We reduce the time spent on a decision by using $w_k = \Delta P/\Delta V$ in the case of MPPT rather than Eq (4), Eq. (5), and (3) as in the original QHBM.

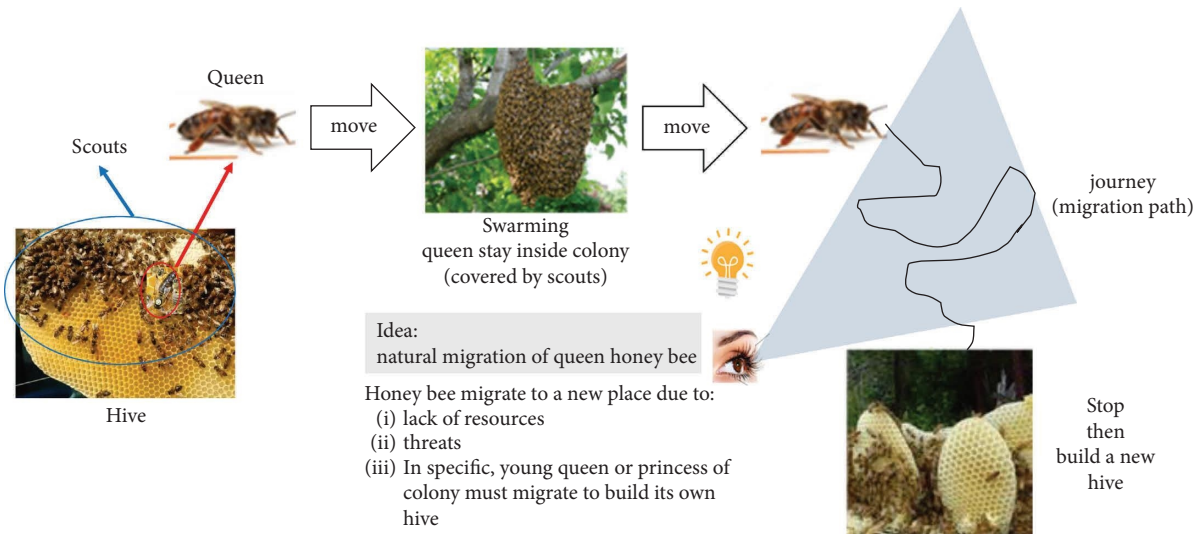

Figure 5: QHBM origin.

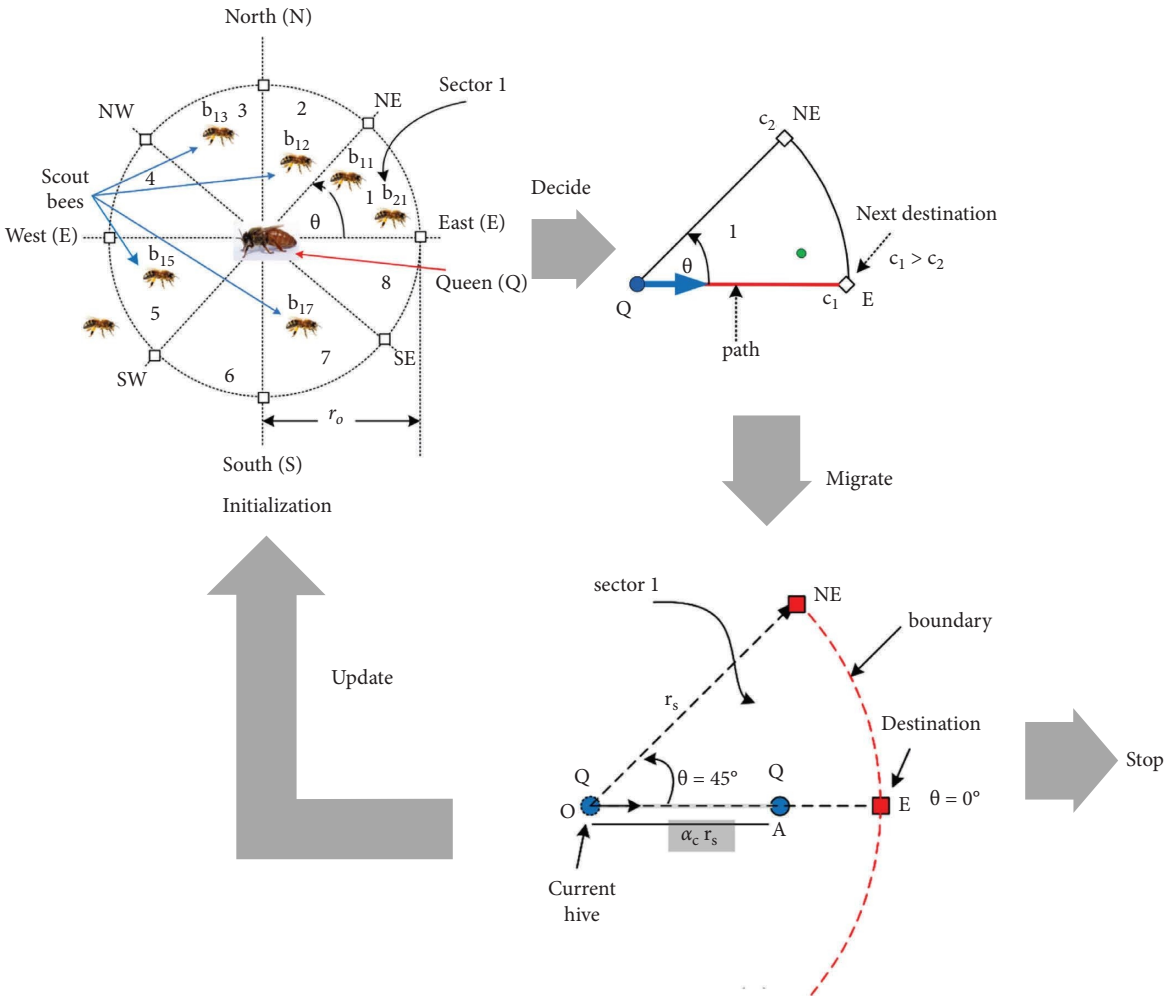

Figure 6: QHBM logical view.

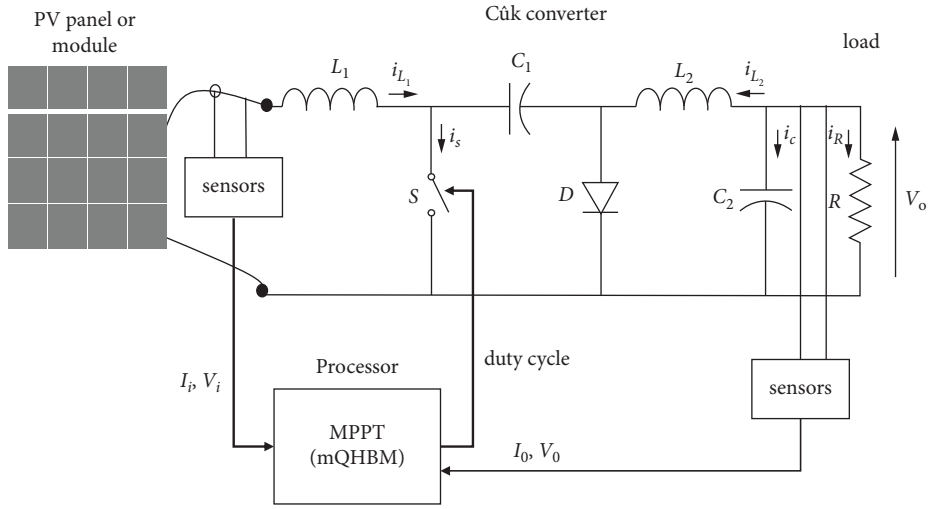

Figure 7: Cûk converter for MPPT.

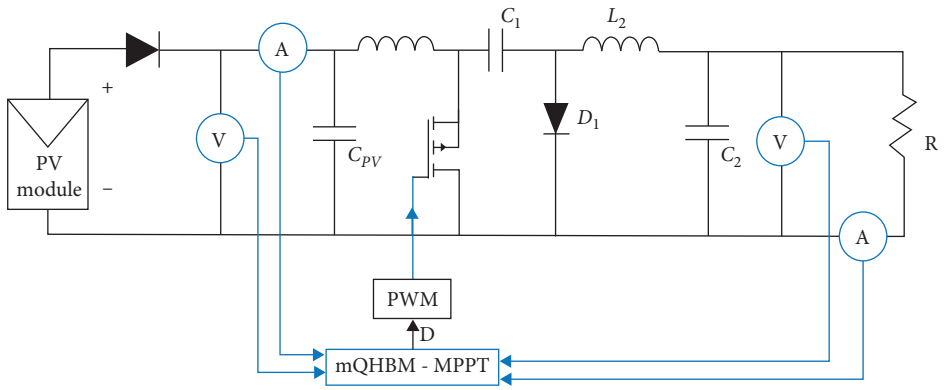

Figure 8: System under study.

Table 1: PV specifications.

Parameter	Value
Open circuit voltage (V_{oc})	21.4 V
Short circuit current (I_{sc})	3.14 A
Maximum power voltage (V_{mp})	17.44 V
Maximum power current (I_{mp})	2.88 A
Maximum power (P_{mpp})	50 Wp

Table 2: Cûk converter.

Parameter	Value
L_1, L_2	3 mH
C_1, C_2	1000 μF
f_s	20 kHz
d	0 to 1

(iii) Change the stopping criterion by (5), so that

$$R_{mpp} - \frac{(1-d)^2}{d^2} R_L \leq 0.01. \quad (11)$$

The workflow of mQHBM in finding MPP is described as follows:

Table 3: Control parameter.

Parameter	Value
K_P	0.31
K_I	1.43
Step size	0.1
ε	0.001

(i) *Initialization.* P_{MPP} is selected for queen destination and given load resistance R_L, queen sight, r is 5.

(ii) The system sensors detect the PV current $I_{Q(k)}$ and PV voltage $V_{Q(k)}$ which are used as the initial coordinates of queen $P_{Q(k)} = V_{Q(k)} * I_{Qk}$, $V_{Q(k)}$. Note that MPPT is a two-dimensional case.

(iii) Scouts are spread randomly in the hotspot regions and their coordinates are $P_{S(k)}, V_{S(k)}$ on P-V curve, respectively.

(iv) The natural factor, α of mQHBM is a random value between 0 and 1. In the mQHBM-based MPPT, the queen decides the weighted information delivered by scout bees in each sector, which is defined as $w(k)$ as follows:

$$w_k = \frac{\Delta P}{\Delta V} = \frac{P_{Q(k)} - \sum_{i=1}^{n} P_{S(k)}}{V_{Q(k)} - \sum_{i=1}^{n} V_{S(k)}}, \quad (12)$$

where k is the current iteration, $P_{Q(k)}$ the current power point, n is the number of scouts bee, and $V_{Q(k)}$ is the queen position that is defined the current measurement of MPP voltage. $V_{S(k)}$ is the scout's position that is defined as the possible GMPP voltage. In terms of mQHBM, the $P_{Q(k)}$, $V_{Q(k)}$ and $P_{S(k)}$, $V_{s(k)}$ are the Queen and Scout's positions on the P-V curve, respectively.

(v) Queen moves to a selected sector and the length of the journey is given by Eq. (6).

(vi) After the queen gets the updated position, the duty cycle (d) value also changes based on the following equation:

$$d = \frac{V_{o(k)}}{V_{0(k)} + V_{Q(k)}}, \quad (13)$$

where $V_{o(k)}$ is the output voltage value obtained from the sensor in the current iteration.

(vii) *Stopping criteria.* The queen decides whether the iteration will be stopped or repeated based on (6).

3.3. Scenarios. The proposed system has been developed, and the simulation was conducted using MATLAB under the following scenarios:

(i) Scenario 1: MPPT simulation on normal irradiation (STC @ 1000 W/m^2).

(ii) Scenario 2: MPPT simulation on sudden changes in irradiation from 1000 W/m^2, 800 W/m^2 to 600 W/m^2. We used the square function to realize this situation, where the interval of each irradiation is 10 seconds.

The data obtained from the respective simulation processes was performed 100 times on average. We compared the accuracy and sensitivity of mQHBM with P&O, PSO, and fuzzy for MPPT under normal and dynamic environments.

4. Simulation Results

We have simulated the system in Figure 8 according to the scenario in Section 3.3. The results are discussed in this section in a separate subsection.

4.1. Case 1: Normal Condition. Under normal conditions, when solar irradiation is 1000 W/m^2, the I–V curve is linear. Observations of each method were carried out 100 times each and the average is shown in Figure 9. Each image has a description of the names of the MPPT methods.

We put the mQHBM method together with one other method on each curve in Figure 9 to see how they compare fairly. In this condition, it is clear that all heuristic algorithms, from traditional ones such as P&O to other more modern algorithms, show satisfactory results. We found the same thing with [1–5, 9, 12], where most heuristic methods converge quickly in the normal case. The difference is in the response speed, convergence speed, and accuracy. All of these heuristic methods do not experience serious oscillations at all and quickly reach their steady state around the MPP.

Compared with the original QHBM, mQHBM is faster to steady state. This is because the learning process is accelerated offline. This will save computation when implemented on a minimal processor. On the other hand, mQHBM compared to other algorithms, is not always the best. When compared with P&O, mQHBM is still much faster to converge, and more accurate than the original QHBM. Likewise, other algorithms, namely PSO, GWO, CS, and ANN, are indeed superior to P&O. This fact had also been found by researchers in the literature [1, 2].

Based on Figure 10, we find that mQHBM is faster towards a steady state than the original QHBM by a difference of 0.04 s. Among all the MPPT heuristic algorithms compared, namely mQHBM, QHBM, P&O, ANN, PSO, GWO, and CS the highest overshoot occurred at P&O at around 1.94 W, and the lowest was at PSO at around 1.04 W. The mQHBM reached 1.07 W greater overshoot than the 0.01 W of original QHBM. GWO, CS, and QHBM only differ slightly, with the highest position of the three being GWO, which reaches 0.25 W. This overshoot is influenced by the computational process of each heuristic technique, so it varies greatly from one to another. The steady-state response speed of all the compared algorithms is almost uniform, where PSO and ANN are the slowest because the computations are the most complex. mQHBM was slightly faster than QHBM in achieving a steady state under normal irradiation conditions.

The accuracy of each method and its computational speed are described in Section 5.1.

4.2. Case 2: Changing Irradiation. The second simulation scenario is carried out by changing the sunlight every 1 s from 1000 W/m^2 to 800 W/m^2 and 600 W/m^2. The results of the MPP stress simulation are shown in Figure 10, where P&O, ANN, PSO, GWO, CS, and mQHBM. In general, all methods experience instantaneous oscillations because the calculation of the target MPP is very small, namely 50 Wp with an MPP voltage of 21.4 V.

Based on the test of changes in sunlight, it was found that mQHBM did not respond too quickly to changes when compared to ANN, PSO, GWO, and CS. In this section, we do not show the power curve because the shape of the image is relatively very similar, so it will be redundant. The interesting thing in this simulation is the oscillation of the MPP voltage. In Figure 10, we see that the P&O strongly oscillates every time there is a change in solar irradiation. ANN, PSO, CS, and GWO are indeed more stable than P&O, as stated [1, 3]. mQHBM is not always better than its competitors, namely ANN, PSO, CS, and GWO. However, it becomes rational that mQHBM is still quite reliable as the choice of normal and shaded MPPT.

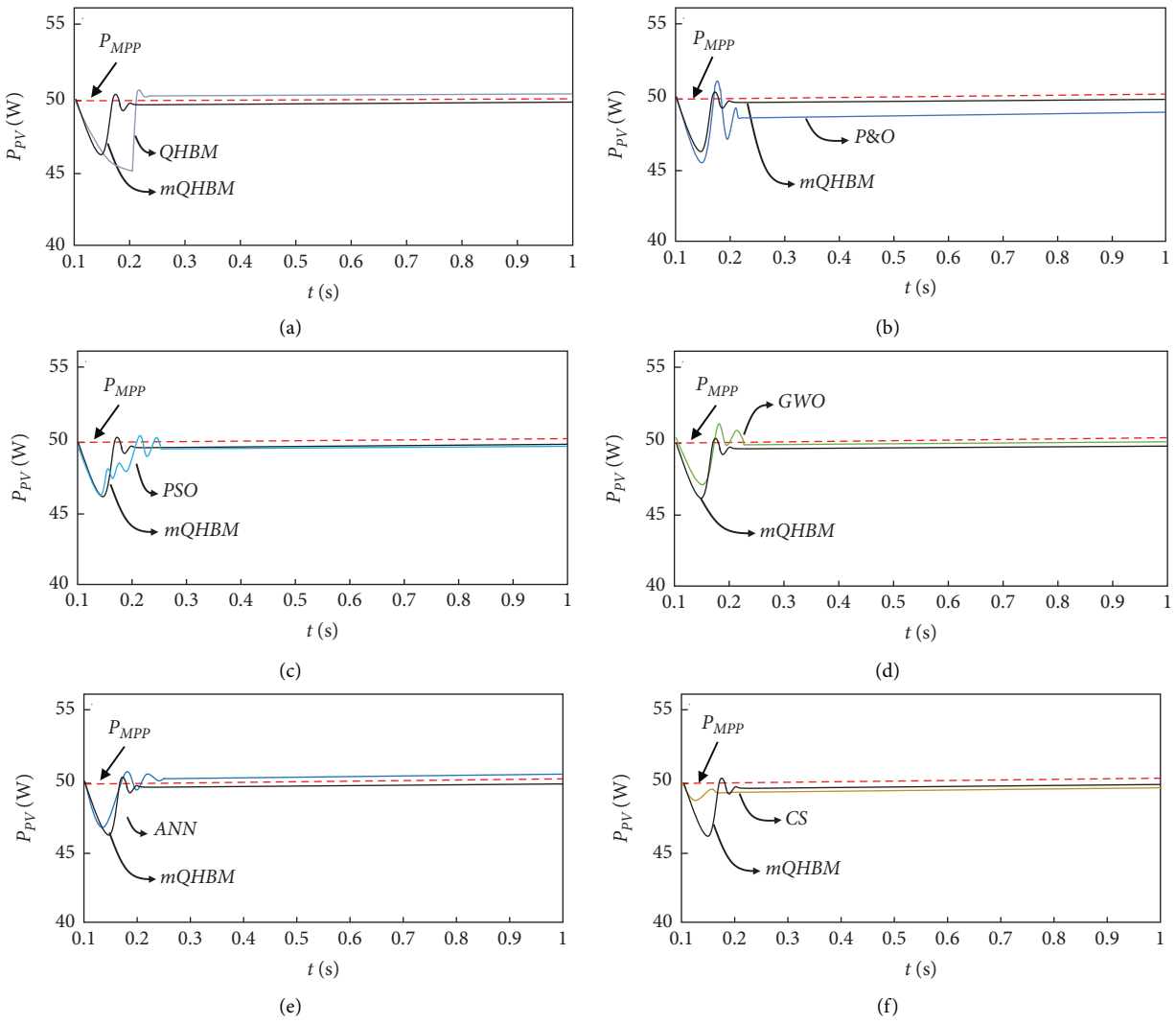

FIGURE 9: PV output power with MPPTs under normal conditions. (a) QHBM vs. mQHBM, (b) mQHBM vs. P&O, (c) mQHBM vs. PSO, (d) mQHBM vs. GWO, (e) mQHBM vs. PSO, and (f) mQHBM vs. GWO.

5. Analysis

5.1. MPPT Accuracy. Figure 11 shows how QHBM traces the PV curve until it finds the MPP in a static environment and the tracking path under dynamic environmental conditions. In a static situation, the mQHBM easily climbs the hill until it finds the MPP point. The tracking path can decrease from peak one to peak two in dynamic environmental conditions, meanwhile, it can be seen that the MPP peak can decrease when the surrounding dynamics occur.

Figure 12 shows one of the conditions when all MPPT methods have determined the final position, where this endpoint is the output power extracted from the solar panel. The difference in output power can be extracted for each method by calculating the absolute error of the MPP. Visually, it can be ascertained that mQHBM has the best accuracy compared to its two rivals, namely PSO and P&O, with errors of 0.03, 1.7, and 0.7, respectively. Thus, the accuracy rates of mQHBM, PSO, and P&O are 99.99%, 97.38%, and 98.54, respectively. An interesting fact is that PSO is not more accurate than P&O in small power applications (50 Wp) because PSO converges faster considering the number of agents or particles used while the step size is not too large.

In the second case, where the solar irradiation was changed intentionally after several seconds, the mQHBM was still the best. The decrease in irradiation level of about 200 W/m^2 in the first interval of 10 seconds and the next interval did not significantly affect the accuracy of mQHBM while PSO and P&O are quite shocked by the accuracy problem when there is a change in solar irradiation. While the mQHBM only decreased by 0.2% and 0.1% accuracy, the PSO accuracy fell by about 6.48% in the first interval and was able to rise again in the next 10 seconds by about 7.9%. Under the same conditions as mQHBM and PSO, P&O accuracy decreased by 0.05% and increased again by 0.66%. The facts above show an anomaly in PSO and P&O when the irradiation decreases.

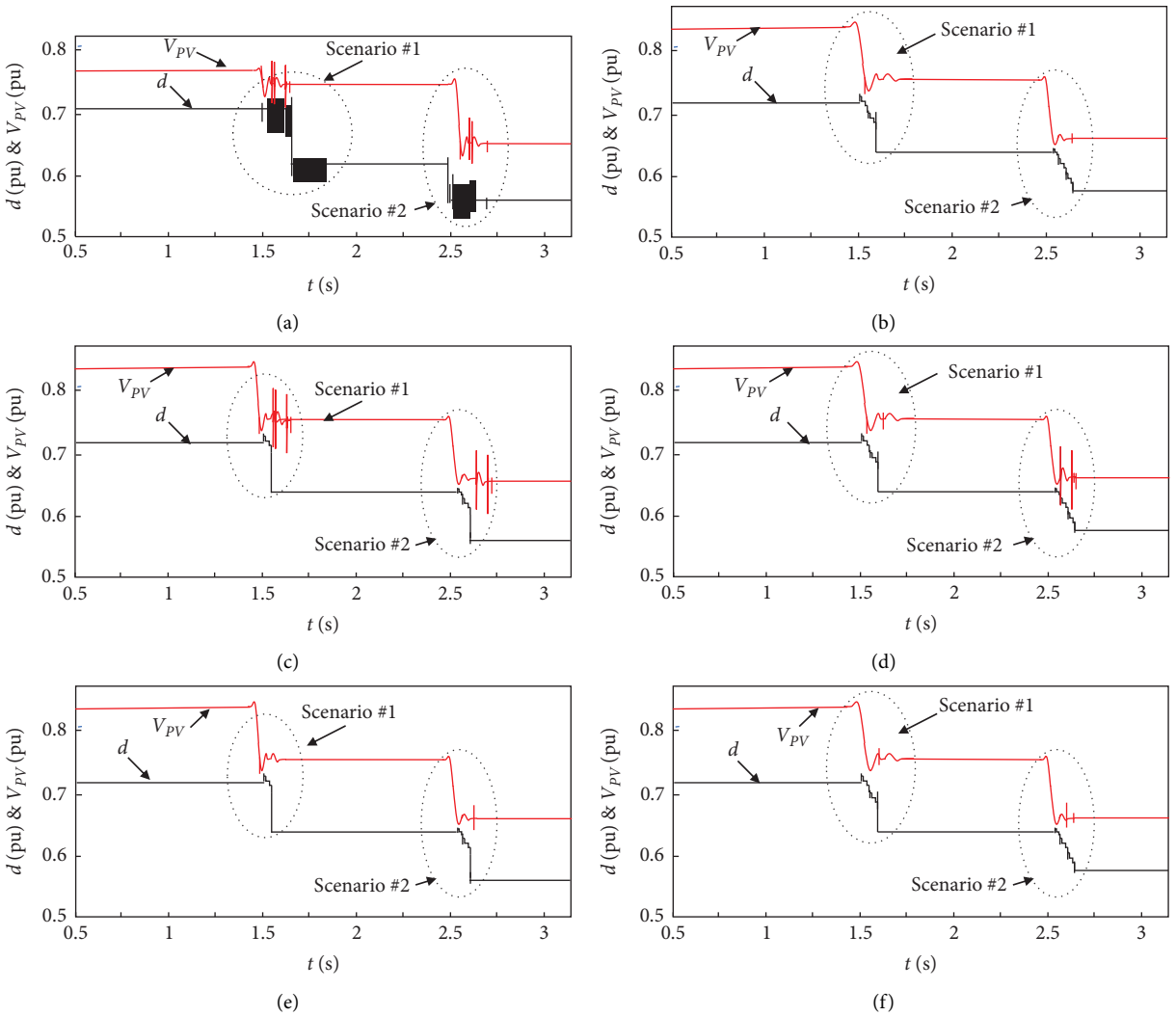

Figure 10: PV output power with MPPTs under shading conditions. (a) P&O, (b) ANN, (c) PSO, (d) GWO, (e) CS, and (f) mQHBM.

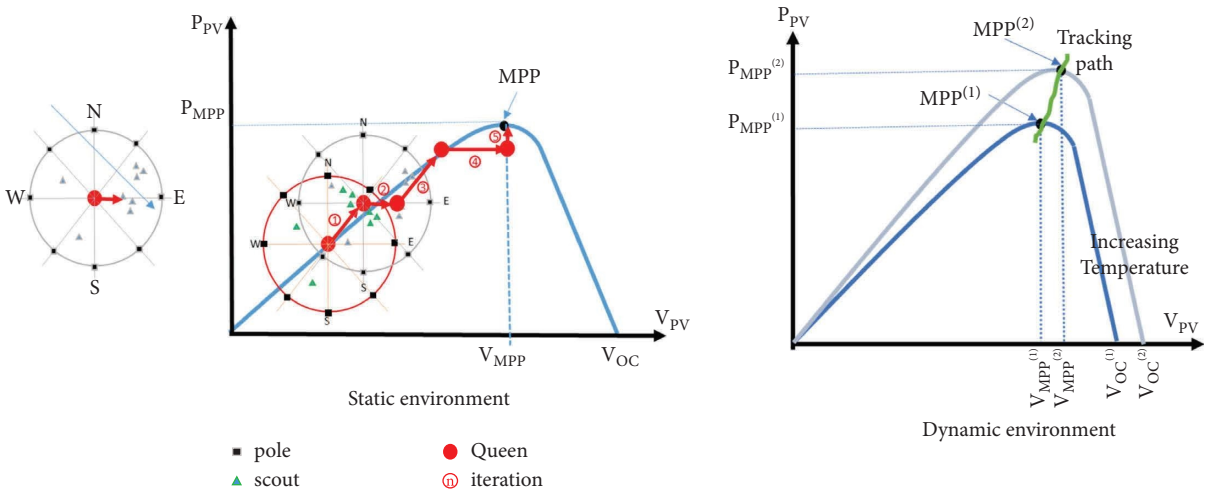

Figure 11: mQHBM search MPP.

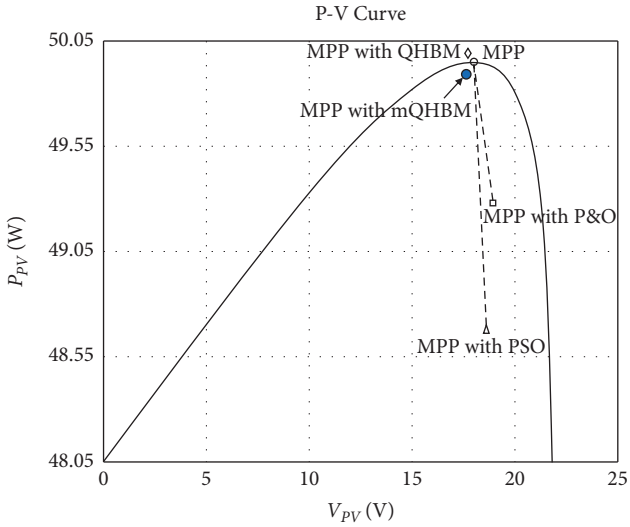

Figure 12: Final position of several MPPTs.

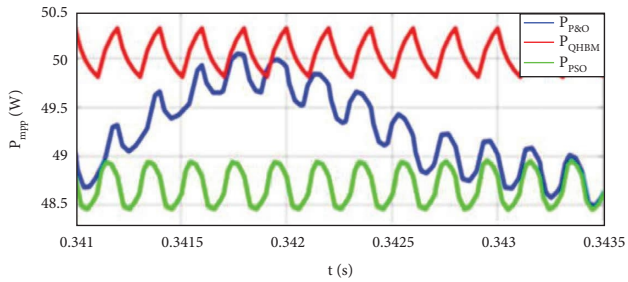

Figure 13: Worst case of tracking oscillation.

5.2. MPPT Response. Based on Tables 4–6, it can be concluded that, in general, the speed of mQHBM in finding MPP in the 1000 W/m^2 normal irradiation case is the fastest. This happens because the desired target has been set at the beginning of the iteration. While PSO is not superior because the random concept used is not suitable for small power 50 Wp. From the outset, P&O had indeed been predicted to be the slowest, as demonstrated by [3] in slightly different applications. Although the difference in MPP tracking time between the three methods is not that large, it is very significant if applied to a low-cost microcontroller.

In the case of irradiation changes, mQHBM was the slowest compared to PSO and P&O, as shown in Tables 4 and 5. This happens because there is a tradeoff between accuracy and speed, where achieving good accuracy, takes a longer time. In the second case (irradiation change), PSO was the fastest compared to mQHBM and P&O. In general, the mQHBM required a longer time when the irradiation decreased while the P&O computation takes a constant time of 0.9 s in response to changes in irradiation. This occurs because the P&O oscillates around the MPP point.

An interesting fact will be seen if we enlarge the curve of the MPP finding to find the oscillations experienced by all MPPT methods before settling MPP. Figure 13 shows three examples of the worst response from PSO, QHBM, and P&O, where this occurs when the transition is shaded from

Table 4: Normal condition.

Method	Irradiation = 1000 W/m^2		
	Power (W)	Time (s)	Accuracy (%)
QHBM	50.11	0.891	99.9989
mQHBM	49.7	0.827	99.97
PSO	48.69	0.835	97.38
P&O	49.27	0.901	98.54
ANN	50.12	0.825	99.9988
GWO	49.98	0.816	99.9998
CS	49.98	0.884	99.9998

Table 5: Scenario #1 of shading condition.

Method	Irradiation = 800 W/m^2		
	Power (W)	Time (s)	Accuracy (%)
QHBM	40.51	0.91	99.9949
mQHBM	39.695	0.88	99.2
PSO	39.36	0.98	90.9
P&O	39.399	0.9	98.49
ANN	40.01	0.1	99.9999
GWO	39.9	0.81	99.999
CS	38.17	0.86	99.9817

Table 6: Scenario #2 of shading condition.

Method	Irradiation = 600 W/m^2		
	Power (W)	Time (s)	Accuracy (%)
QHBM	29.01	1.12	99.9901
mQHBM	29.755	0.94	99.1
PSO	29.64	0.7	98.8
P&O	29.35	0.9	97.83
ANN	30	2	100
GWO	29	0.91	99.99
CS	29.1	1.23	99.991

1000 W/m^2 to 800 W/m^2. P&O was not accurate, and at worst, it could be seen that P&O oscillated towards LMPP, then climbed again to GMPP, and then dropped away from LMPP. This incident shows that P&O was not able to properly track MPP. PSO also oscillates at its worst and reaches hysterics around the GMPP. This is because many particle agents respond to the sudden transition from normal to shaded. As with P&O and PSO at their worst, QHBM also oscillates, but QHBM is closer to GMPP by a 0.5 W margin than MPP. The QHBM is hysterical around the MPP as the released scout's agent responds to changes in irradiation and attempts to provide information to Queen. Queen received info from another scout agency and decided to return to GMPP. This is no longer the case with mQHBM with the aforementioned modifications.

6. Conclusion

We have successfully developed mQHBM and tested this method for tracking MPP on a 50 Wp PV system. A fair comparison with several well-known heuristic methods, namely the original QHBM, ANN, PSO, GWo, CS, and

traditional HC, namely P&O, has been carried out in two cases, namely normal irradiation conditions and changes in irradiation (shaded) reliable in normal cases.

We recognize that mQHBM is not always the best, given its shortened stages. However, for implementation at a minimum, this system is good. The mQHBM takes a longer time than PSO, GWO, QHBM, ANN, and CS. Even so, the mQHBM can still be relied on in terms of accuracy, which always reaches above 98% or more in all conditions. The advantage of mQHBM is that it determines the MPP target from the beginning, thereby reducing errors in determining the MPP where the original QHBM takes a longer time, as is the case with PSO, P&O, and other competitors.

In the future, we will further improve the performance of the mQHBM and observe the shaded transition. The shaded transition is a dynamic process because it is influenced by changes in the weather, dust, etc. The performance of mQHBM under changing loads will be observed as a major project in the future, especially on solar power systems for charging stations and building integrated PV systems.

Data Availability

No data are available to support the findings of this study.

Conflicts of Interest

The authors declare that they have no conflicts of interest regarding this paper.

Acknowledgments

This work was supported by PNBP UM, Indonesia with contract 20.3.42/UN32.14.1/LT/2020.

References

[1] K. Yung Yap, C. R. Sarimuthu, and J. Mun-Yee Lim, "Artificial intelligence based MPPT techniques for solar power system: a review," *Journal of Modern Power Systems and Clean Energy*, vol. 8, no. 6, pp. 1043–1059, November 2020.

[2] R. B. Bollipo, S. Mikkili, and P. K. Bonthagorla, "Hybrid, optimal, intelligent and classical PV MPPT techniques: a review," *CSEE Journal of Power and Energy Systems*, vol. 7, no. 1, pp. 9–33, 2021.

[3] B. Bendib, H. Belmili, and F. Krim, "A survey of the most used MPPT methods: conventional and advanced algorithms applied for photovoltaic systems," *Renewable and Sustainable Energy Reviews*, vol. 45, pp. 637–648, 2015.

[4] L. M. Elobaid, A. K. Abdelsalam, and E. E. Zakzouk, "Artificial neural network-based photovoltaic maximum power point tracking techniques: a survey," *IET Renewable Power Generation*, vol. 9, no. 8, pp. 1043–1063, 2015.

[5] S. Allahabadi, H. Iman-Eini, and S. Farhangi, "Fast artificial neural network based method for estimation of the global maximum power point in photovoltaic systems," *IEEE Transactions on Industrial Electronics*, vol. 69, no. 6, pp. 5879–5888, 2022.

[6] S. R. Kiran, C. H. H. Basha, V. P. Singh, C. Dhanamjayulu, B. R. Prusty, and B. Khan, "Reduced simulative performance analysis of variable step size ANN based MPPT techniques for partially shaded solar PV systems," *IEEE Access*, vol. 10, Article ID 48875, 2022.

[7] M. Kermadi, Z. Salam, J. Ahmed, and E. M. Berkouk, "An effective hybrid maximum power point tracker of photovoltaic arrays for complex partial shading conditions," *IEEE Transactions on Industrial Electronics*, vol. 66, no. 9, pp. 6990–7000, 2019.

[8] M. Dehghani, M. Taghipour, G. B Gharehpetian, and M. Abedi, "Optimized Fuzzy controller for MPPT of grid-connected PV systems in rapidly changing atmospheric conditions," *Journal of Modern Power Systems and Clean Energy*, vol. 9, no. 2, pp. 376–383, 2021.

[9] S. Jalali Zand, S. Mobayen, H. Z. Gul, H. Molashahi, M. Nasiri, and A. Fekih, "Optimized Fuzzy controller based on Cuckoo optimization algorithm for maximum power-point tracking of photovoltaic systems," *IEEE Access*, vol. 10, Article ID 71699, 2022.

[10] R. Iftikhar, I. Ahmad, M. Arsalan, N. Naz, N. Ali, and H. Armghan, "MPPT for photovoltaic system using nonlinear controller," *International Journal of Photoenergy*, vol. 2018, Article ID 6979723, 11 pages, 2018.

[11] S. Obukhov, A. Ibrahim, A. A. Zaki Diab, A. S. Al-Sumaiti, and R. Aboelsaud, "Optimal performance of dynamic particle swarm optimization based maximum power trackers for stand-alone PV system under partial shading conditions," *IEEE Access*, vol. 8, Article ID 20770, 2020.

[12] S. Javed, K. Ishaque, S. A. Siddique, and Z. Salam, "A simple yet fully adaptive PSO algorithm for global peak tracking of photovoltaic array under partial shading conditions," *IEEE Transactions on Industrial Electronics*, vol. 69, no. 6, pp. 5922–5930, June 2022.

[13] S. Makhloufi and S. Mekhilef, "Logarithmic PSO-based global/local maximum power point tracker for partially shaded photovoltaic systems," *IEEE Journal of Emerging and Selected Topics in Power Electronics*, vol. 10, no. 1, pp. 375–386, Feb. 2022.

[14] M. Joisher, D. Singh, S. Taheri, D. R. Espinoza-Trejo, E. Pouresmaeil, and H. Taheri, "A hybrid evolutionary-based MPPT for photovoltaic systems under partial shading conditions," *IEEE Access*, vol. 8, Article ID 38481, 2020.

[15] K. Hu, S. Cao, W. Li, and F. Zhu, "An improved particle swarm optimization algorithm suitable for photovoltaic power tracking under partial shading conditions," *IEEE Access*, vol. 7, Article ID 143217, 2019.

[16] S. Figueiredo and R. Nayana Alencar Leão e Silva Aquino, "Hybrid MPPT technique PSO-P&O applied to photovoltaic systems under uniform and partial shading conditions," *IEEE Latin America Transactions*, vol. 19, no. 10, pp. 1610–1617, Oct, 2021.

[17] J. P. Ram, D. S. Pillai, N. Rajasekar, and S. M. Strachan, "Detection and identification of global maximum power point operation in solar PV applications using a hybrid ELPSO-P&O tracking technique," *IEEE Journal of Emerging and Selected Topics in Power Electronics*, vol. 8, no. 2, pp. 1361–1374, 2020.

[18] K. Sundareswaran, V. Vignesh kumar, and S. Palani, "Application of a combined particle swarm optimization and perturb and observe method for MPPT in PV systems under partial shading conditions," *Renewable Energy*, vol. 75, pp. 308–317, 2015.

[19] I. Pervez, I. Shams, S. Mekhilef, A. Sarwar, M. Tariq, and B. Alamri, "Most valuable player algorithm based maximum power point tracking for a partially shaded PV generation system," *IEEE Transactions on Sustainable Energy*, vol. 12, no. 4, pp. 1876–1890, 2021.

[20] S. Mohanty, B. Subudhi, and P. K. Ray, "A new MPPT design using grey wolf optimization technique for photovoltaic system under partial shading conditions," *IEEE Transactions on Sustainable Energy*, vol. 7, no. 1, pp. 181–188, 2016.

[21] K. Guo, L. Cui, M. Mao, L. Zhou, and Q. Zhang, "An improved Gray wolf optimizer MPPT algorithm for PV system with BFBIC converter under partial shading," *IEEE Access*, vol. 8, Article ID 103476, 2020.

[22] I. S. Millah, P. C. Chang, D. F. Teshome, R. K. Subroto, K. L. Lian, and J.-F. Lin, "An enhanced grey wolf optimization algorithm for photovoltaic maximum power point tracking control under partial shading conditions," *IEEE Open Journal of the Industrial Electronics Society*, vol. 3, pp. 392–408, 2022.

[23] C. Y. Liao, R. K. Subroto, I. S. Millah, K. L. Lian, and W.-T. Huang, "An improved bat algorithm for more efficient and faster maximum power point tracking for a photovoltaic system under partial shading conditions," *IEEE Access*, vol. 8, Article ID 96378, 2020.

[24] D. A. Nugraha, K. L. Lian, and Suwarno, "A novel MPPT method based on Cuckoo search algorithm and golden section search algorithm for partially shaded PV system," *Canadian Journal of Electrical and Computer Engineering*, vol. 42, no. 3, pp. 173–182, 2019.

[25] G. Jong and G. Horng, "A novel queen honey bee migration (QHBM)," *Wireless Personal Communications*, vol. 95, no. 3, pp. 3209–3232, 2017.

[26] H. Wibowo, "A new MPPT based on queen honey bee migration (QHBM) in stand-alone photovoltaic," in *Proceedings of the 2019 IEEE Int. Conf. Autom. Control Intell. System*, pp. 123–128, Selangor, Malaysia, June 2019.

[27] S. Titri, C. Larbes, K. Toumi, and K. Benatchba, "A new MPPT controller based on the Ant colony optimization algorithm for photovoltaic systems under partial shading conditions," *Applied Soft Computing*, vol. 58, 2017.

[28] K. Sundareswaran, P. Sankar, P. S. R. Nayak, S. P. Simon, and S. Palani, "Enhanced energy output from a PV system under partial shaded conditions through artificial bee colony," *IEEE Transactions on Sustainable Energy*, vol. 6, no. 1, pp. 198–209, 2015.

[29] N. Singh, K. K. Gupta, S. K. Jain, N. K. Dewangan, and P. Bhatnagar, "A flying Squirrel search optimization for MPPT under partial shaded photovoltaic system," *IEEE Journal of Emerging and Selected Topics in Power Electronics*, vol. 9, no. 4, pp. 4963–4978, 2021.

[30] S. Lyden, H. Galligan, and M. E. Haque, "A hybrid simulated annealing and perturb and observe maximum power point tracking method," *IEEE Systems Journal*, vol. 15, no. 3, pp. 4325–4333, 2021.

[31] K. Nathan, S. Ghosh, Y. Siwakoti, and T. Long, "A new DC-DC converter for photovoltaic systems: coupled-inductors combined cûk-SEPIC converter," *IEEE Transactions on Energy Conversion*, vol. 34, no. 1, pp. 191–201, 2019.

[32] M. Lakshmi and S. Hemamalini, "Nonisolated high gain DC-DC converter for DC microgrids," *IEEE Transactions on Industrial Electronics*, vol. 65, no. 2, pp. 1205–1212, 2018.

[33] D. G and S. N. Singh, "Selection of non-isolated DC-DC converters for solar photovoltaic system," *Renewable and Sustainable Energy Reviews*, vol. 76, pp. 1230–1247, 2017.

[34] S. Hosseini, S. Taheri, M. Farzaneh, and H. Taheri, "A high-performance shade-tolerant MPPT based on current-mode control," *IEEE Transactions on Power Electronics*, vol. 34, no. 10, Article ID 10327, 2019.